

Serveur Académique Lausannois SERVAL serval.unil.ch

Author Manuscript

Faculty of Biology and Medicine Publication

This paper has been peer-reviewed but does not include the final publisher proof-corrections or journal pagination.

Published in final edited form as:

Title: Polycyclic aromatic hydrocarbons (PAHs) skin permeation rates change with simultaneous exposures to solar ultraviolet radiation (UV-S)

Authors: Hopf NB, Spring P, Hirt-Burri N, Jimenez S, Sutter B, Vernez D, Berthet A

Journal: Toxicology Letters

Year: 2018

Issue: 287

Pages: 122-130

DOI: [10.1016/j.toxlet.2018.01.024](https://doi.org/10.1016/j.toxlet.2018.01.024)

In the absence of a copyright statement, users should assume that standard copyright protection applies, unless the article contains an explicit statement to the contrary. In case of doubt, contact the journal publisher to verify the copyright status of an article.

Polycyclic aromatic hydrocarbons (PAHs) skin permeation rates change with simultaneous exposures to solar ultraviolet radiation (UV-S)

Nancy B Hopf¹, Philipp Spring², Nathalie Hirt-Burri³, Silvia Jimenez¹, Benjamin Sutter⁴, David Vernez¹, Aurelie Berthet¹.

¹ Institute for Work and Health (IST), Universities of Lausanne and Geneva, Lausanne-Epalinges, Switzerland. Nancy.Hopf@hospvd.ch; Aurelie.Berthet@hospvd.ch; David.Vernez@hospvd.ch;

² Centre Hospitalier Universitaire Vaudois (CHUV), Department of Dermatology, Lausanne, Switzerland. Philipp.Spring@chuv.ch;

³ Centre Hospitalier Universitaire Vaudois (CHUV), Department of Musculoskeletal Medicine (DAL), Lausanne, Switzerland. Nathalie.Burri@chuv.ch

⁴ Institut National de Recherche et de Securite (INRS), Vandoeuvre Cedex, France. benjamin.sutter@inrs.fr

Corresponding author:

Nancy B. Hopf, Ph.D.

Institute for Work and Health (IST), Route de la Corniche 2, CH-1066 Lausanne-Epalinges, Switzerland. Phone: +41 (0) 21 314 9558 Fax: +41 (0) 21 314 7430. Nancy.Hopf@hospvd.ch

Journal: Toxicological letters

Abstract: 197 words

No. tables: 1

No. figures: 3

KEY words: Polycyclic aromatic hydrocarbons; PAH; skin permeation; skin exposure; solar ultraviolet radiation; UV; human skin; bitumen; flow-through diffusion cells;

Abstract

Road construction workers are simultaneously exposed to two carcinogens; solar ultraviolet (UV-S) radiation and polycyclic aromatic hydrocarbons (PAHs) in bitumen emissions. The combined exposure may lead to photogenotoxicity and enhanced PAH skin permeation rates. Skin permeation rates (J) for selected PAHs in a mixture (PAH-mix) or in bitumen fume condensate (BFC) with and without UV-S co-exposures were measured with in vitro flow-through diffusion cells mounted with human viable skin and results compared. Possible biomarkers were explored. *J*s were greater with UV-S for naphthalene, anthracene, and pyrene in BFC (0.08-0.1ng/cm²/h) compared to without (0.02-0.26ng/cm²/h). This was true for anthracene, pyrene, and chrysene in the PAH-mix. Naphthalene and benzo(a)pyrene (BaP) in the PAH-mix had greater *J*s *without* (0.97-13.01ng/cm²/h) compared to *with* UV-S (0.40-6.35ng/cm²/h). Time until permeation (T_{lags}) in the PAH-mix were generally shorter compared to the BFC, and they ranged from 1 to 13h. The vehicle matrix could potentially be the reason for this discrepancy as BFC contains additional not identified substances. Qualitative interpretation of p53 suggested a dose-response with UV-S, and somewhat with the co-exposures. MMP1, p65 and cKIT were not exploitable. Although not statistically different, PAHs permeate human viable skin faster with simultaneous exposures to UV.

Introduction

Simultaneous exposures to two carcinogens; polycyclic aromatic hydrocarbons (PAHs) and solar ultraviolet radiation (UV-S) are common among road pavers; a world-wide activity involving tens of thousands of workers (IARC 2013). Pavers work outside (UV-S exposures) handling hot straight-run bitumen containing PAHs. The International Agency for Research on Cancer (IARC) concluded in 2013 that occupational exposures to paving bitumen (CAS no. 8052-42-4) and their emissions during road paving are possibly carcinogenic to humans (Group 2B) (IARC 2013).

Road paving workers are not only exposed via inhalation, but to a large extent via skin which in combination with UV-S exposures can increase the risk of skin cancer (Burke and Wei 2009). The synergistic mechanism for this is not known. The extent of skin exposures to bitumen (or asphalt) among road paving workers depends on the tasks performed; pavers – drive the paver machine distributing the asphalt (bitumen and gravel mix), screed operators – controls the even spread of asphalt behind the paving machine, rakers – move the excess bitumen to fill in voids and prepare joints for rolling, and rollers – drive the machinery that compacts the asphalt mat. The surface contamination of the tools will also add to the overall skin exposures.

The PAH concentrations in bitumen fume increase with the temperature (Boilliet et al. 2015; Cavallari et al. 2012; Lange et al. 2007). To reduce the amount of PAHs in bitumen, the paving material is generally heated to only 180°C. Bitumen fume condensates (BFCs) have been analyzed for PAH content, and typical PAHs found were (listed by name and IARC category): naphthalene (cat. 2B), acenaphthylene (cat. not assessed), acenaphthene (cat. 3), phenanthrene (cat. 3), anthracene (cat. 3), fluoranthene (cat. 3), pyrene (cat. 3), benzo[a]anthracene (cat. 2B), chrysene (cat. 2B), and benzo[a]pyrene (BaP) (cat.1) (reviewed in (Binet et al. 2002)).

Sunlight (UV-S) is a carcinogen and the main cause of skin cancer development (IARC 1992; Rass and Reichrath 2008). The solar radiation is composed of 91% visible (400-700 nm), 8.7% UVA (320-400 nm), and 0.3% UVB (280-320 nm). It is known that UVA acts on endogenous photosensitizers to form free radicals, which subsequently damage DNA, cell membranes, and other cellular constituents (Burke and Wei 2009). UVB induces immunosuppression while UVA does not. UVA penetrates the full epidermis and dermis and decreases the skin's protective immune response, thereby decreasing natural recognition and elimination of cells genetically damaged by

UVB (Garssen and van Loveren 2001). Quantities of UV radiation are expressed using radiometric terminology, and measured in clinical terms as the standard erythemal dose (SED); a measure of the erythemal effectiveness of UV exposure. UVA is less erythrogenic and carcinogenic than UVB. It is not known what UVA and UVB doses cause cancers.

PAHs are photosensitizers and absorb sunlight in the UVA range thereby becoming excited to upper energy states (reviewed in (Yu 2002)). These can undergo electron or energy transfers to molecular oxygen, solvents, or biological molecules in the cell and generate reactive oxygen species (ROS). A ROS pathway has been proposed (Burke and Wei 2009) as a likely cancer mechanism. It is generally recognized that oxidative stress is associated with p53-dependent cell cycle arrest. The p53 gene can also be induced by BaP diol epoxide; the BaP metabolite recognized as the ultimate carcinogen, in human epithelial cells (Perlow et al. 2002). Another, not yet tested hypothesis is that PAHs are absorbed through skin at a greater extent because UV-S exposures break down the skin's structure (Lahmann et al. 2001; Scharffetter et al. 1991) leading to a more permeable skin barrier. For instance, skin penetration enhancement after solar irradiation has been observed in assays with caffeine (Gelis et al. 2002).

Even at PAH concentrations below the toxic or tumorigenic levels, the combined impact of the two factors; UV-S and PAHs, may contribute to an increased tumorigenicity in animals (Liu et al. 1998; Saladi et al. 2003; Shyong et al. 2003; Wang, Saladi, and Wei 2003). Exposure to BaP and UVA synergistically induced oxidative DNA damage (Liu et al. 1998; Saladi et al. 2003; Shyong et al. 2003). This can enhance the mutational potential of genes such as ras and p53; genes that activate signal transduction pathways and protective enzymes (Saladi et al. 2003). From this activation, p53 would be expected to be upregulated. UVB can also increase the keratinocytes' production stem cell factor (SCF). SCFs bind to the tyrosine-protein kinase (cKIT) on the melanocytes and result in receptor dimerization and activation of protein kinase activity (Roskoski 2005; Yoshida et al. 2001). An increase in SCF would induce the production of cKIT receptors. UVB can also induce the regulation of cell survival and proliferation in melanogenesis directly by increasing cKIT receptors (Hachiya et al. 2001). As a result, cKIT would be expected to be upregulated. Δ NP63 α (the p63 isoform lacking the transcription activation domain) is a member of the p53 family of transcription factors and is essential for epithelial maintenance and epidermal morphogenesis (Mills et al. 1999; Yang et al. 1998). Δ NP63 α is expressed in keratinocytes and acts as a critical proliferative factor (Senoo et al.

2007). With an induced proliferation, Δ NP63 α is expected to be downregulated. The interstitial collagenase (also known as matrix metalloproteinase 1 or MMP-1) is responsible for maintaining the dermal extracellular matrix structure. The observed disorganization and degeneration of dermal extracellular matrix in UV exposed skin is due to an increased MMP-1 production (Lahmann et al. 2001; Scharffetter et al. 1991).

Combined skin exposures to PAHs and UV-S and their impact on PAH absorption have until now not been well assessed. The *in vitro* flow-through diffusion cell system is suitable to study skin absorption *ex vivo*. The diffusion cell is separated into two chambers with a skin flap; the upper donor chamber (concentration of selected PAHs) and a lower receiver compartment with a continuous flow of liquid. The cumulative PAH concentrations in the receiver compartment is plotted over 24 hours; this permeation curve is used to calculate absorption rates across the skin. In this *in vitro* study, we characterized permeation of PAHs across human viable skin applied as a mixture and as BFC with and without simultaneous UV-S exposures. Our hypothesis was that in this experimental design, human skin permeation rates (J) and time until permeation across the skin barrier (T_{lag}) would be significantly different between skin exposed to PAHs alone and PAHs with simultaneous co-exposures to UV-S. We also explored possible skin biomarkers for UV exposures such as p53, Δ NP63 α , cKIT, and MMP1. Understanding PAH skin absorption when co-exposure to UV-S is present can provide insight into internal PAH dose and consequently carcinogenic potential. The skin permeation parameters can be used to estimate the body burden in order to evaluate phototoxic responses based on PAH dose.

Methods

Chemicals Naphthalene (CAS no. 91-20-1), anthracene (CAS no.120-12-7), pyrene (CAS no. 129-00-0), chrysene (CAS no. 218-01-9), and benzo[a]pyrene (CAS no. 50-32-8) were purchased from Sigma Aldrich (Buchs, Switzerland). A standard mixture was made adding 5 mg/ml of each PAH in acetone, this is referred to as the “PAH mix”. Polyoxyethylene oleyl ether (Brij®-98, CAS no. 9004-98-2) was purchased from SigmaAldrich (Switzerland).

Bitumen fume generation. The fume from obtained road construction bitumen (CAS 8052-42-4; CTW-Strassenbaustoffe AG, Switzerland) was generated in a week long process. Information regarding the bitumen fume generator itself has been described previously (Sutter et al. 2016). Briefly, the bitumen was heated in a vessel to 170°

C, and fume collected in a condensation system, before extraction with dichloromethane. Dichloromethane was gently evaporated until the BFC weight reduction was stable. Seven days of continued generation gave 2-4 mL of BFC, which was diluted in toluene and shipped to the skin experiment laboratory.

Solar light lamp. A 1000W xenon lamp (Solar LIGHT® Model LS-1000-4S-009 Solar Simulator, Glenside, Pennsylvania, USA) was used for the experiments. The UV-S spectrum comprised of 9.5% UVB and 90.5% UVA, closely matching the spectrum of natural sunlight (Diffey 2002). The standard erythemal dose (SED), which is equivalent to 100 J/m², was measured with an erythema dose detector (Solar Light radiometer PMA2100 equipped with PMA2101S S/N: 17789). Exposure times chosen for the experiments were either 10-15 minutes equal to 22.5-30 mJ/cm² (2-3 SED) and 40 minutes equal to 60 mJ/cm² (6 SED). In other words, a 10 min exposure from this UV lamp could give a sunburn in a person with very sensitive skin. For the comparison with outdoor measurements, given that it is not linear over the day and that it is dependent on the weather, could be interpreted as exposure during sunbathing (horizontal to the ground) at noon in the summer for 1 hour (Milon et al. 2007).

Human skin. Surgically removed skin from patients (N=10; where five donor skins were used for skin permeation studies and five for histological examination) undergoing abdominoplasty at the Lausanne university hospital (CHUV). Skin was obtained from the Department of Musculoskeletal Medicine (DAL) biobank, under anonymous donation, in accordance with its regulation and accepted by the cantonal ethics committee under protocol 264/12. No more than two hours elapsed from time of surgery-end to the skin was mounted onto the flow-through diffusion cells. No personal parameters regarding the patients were retained.

Flow-through diffusion cell experiments. The skin was dermatomed (Acculan®II, B. Braun/Aesculap, Sempach, Switzerland) to a thickness of 800 µm, and the skin discs mounted onto the flow-through diffusion cells. A rack of six jacketed flow-through diffusion cells (receptor volume 12 mL; PermaGear bought from SES Analytical System, Bechenheim, Germany) was operated at 32°C. For the permeation studies, the peristaltic pump (Ismatec IPC-N, IDEX Health & Science GmbH, Wertheim-Mondfeld, Germany) ran at a flow rate of 40 µl/min, and a fraction collector (FC 204, Gilson Inc., Middleton, WI, USA) automatically sampled the reservoir liquid; saline solution with 6% Brij®. For the skin biomarker studies, the system was operated in static mode. To keep the skin nourished throughout the 24h experiment, the reservoir liquid was Dulbecco's Modified Eagle's Medium (DMEM D6429 from Aldrich-Sigma, Switzerland). Skin was considered stabilized when the trans epidermal water loss (TEWL)

(VapoMeter wireless, Delfin Technologies Ltd., Kuopio, Finland) readings were stable and below 11 g/m²/h (Pinnagoda et al. 1990). If TEWL were above this value, the skin discs were deemed damaged and replaced. The exposed skin area was 1.77 cm². A sample of the PAH mixture (60 µL) or BFC (60 µL) was added to the mounted skin and the UV-S exposure applied with a dose equivalent to six SED (60 mJ/cm²). This applied amount corresponds to infinite dose. The cells were run in duplicate or triplicate depending on amount of donor skin for each exposure (PAH with or without UV-S) and controls. The automated sampling collection was set for intervals lasting 24 hours. Samples were collected in brown glass vials as PAHs are sensitive to light. Our study complies with the OECD guideline 428 in: describing the skin origin, skin preparation, proof of skin integrity using the TEWL, temperature (32°C), the choice of a suitable receptor fluid, the description of the diffusion cells used, the actual area of skin dosed, the number of cells/samples and donors, the duration of sampling period (24h). We did not include the determination of the PAH amount retained in skin after washing.

Chemical analysis. PAH concentrations were determined for the bitumen condensate (Table 1) used in the experiments. The brown collection vials from the flow-through diffusion cell experiments were extracted before analysis. The extraction method has already been published (Huynh et al. 2007). Briefly, the solid phase extraction column (SPE; HyperSep C18, 500 mg, 6 ml) was conditioned (methanol (5 ml) and washed with water (5 ml)). The total sampled volume was added and washed twice with water (5 ml). The PAHs were eluted with ethyl acetate (5 ml), dried, and reconstituted in acetonitrile (500 µl). Samples were injected into a high performance liquid chromatograph (HPLC) and analytically separated on a capillary column (Pinnacle II, PAH, 4 µm 150 x 3,2 mm) at 30°C, 1.3 ml/min and with a mobile phase A (water:acetonitril 50:50) and B (100% acetonitril) with the following %A:%B gradient: 0 min 80:20, 3 min 80:20, 10 min 0:100, and 15 min 0:100. The analytes were detected and quantified by fluorescence (ProStar 363) with the following excitation (λ_{ex}) and emission (λ_{em}) wavelengths (nm); naphthalene λ_{ex} 280 λ_{em} 340, anthracene λ_{ex} 250 λ_{em} 376, pyrene λ_{ex} 333 λ_{em} 382, chrysene λ_{ex} 280 λ_{em} 378, and benzo(a)pyrene λ_{ex} 296 λ_{em} 405. The quantification limits were from 10-20 ng/mL for the five PAHs.

Data analysis. Permeability coefficients (Kp) were estimated from the slopes of the cumulative absorption plots over time. Lag times (τ) were estimated as the intercept of the steady state portion of the permeability rate (J) curves with the time axis. Individual permeation rates were calculated from each diffusion cell and the mean and standard deviations were calculated for the group. Kp was estimated by dividing J with the applied concentration.

Gene expression biomarkers. The skin was irradiated with the lamp for 15-20 or 40 minutes which is equivalent to a sun exposure of 3-4 or 8 hrs in Switzerland. Several incubation times after exposure were tested: 0, 1h and 24 hrs. After an incubation period of 1 or 24 hrs, the skin sections were removed from the flow-through diffusion cells and cut to keep only the most central part of the skin. All skin samples were sent for routine pathological staining analyses. The paraffin-embedded and formalin-fixed skin were stained for immunohistochemistry using normal hematoxylin-eosin (H&E) staining; p53 expression with monoclonal mouse Anti-human P53 protein, clone DO-7 (as described in (Fonseca et al. 2016)); p63 expression with mouse monoclonal, clone DAK-p63, core DNA-binding domain of human p63 protein reacting with TAp63 and Δ Np63 isoforms of p63); cKit/CD117 expression with rabbit polyclonal.

The histology slides were analyzed using a microscope (Nikon 90i) with an integrated camera. Each image was studied in 10x, 40x, and 100x resolution. Signs of irritation and cell damage were categorized on the hematoxyline eosin (HE) staining, in particular the accumulation of fluid between the keratinocytes in the epidermis (spongiosis) and vacuolization of the basal epidermal layer (epidermolysis) (Miles et al. 2014). The p53 grading was performed single-blinded by a dermatopathology medical doctor. We defined the intensity of p53 in four quantitative stages (none, weak, middle, strong) and qualitatively by color (none, clear, brown, dark). The low quantitative stage was graded from five “hot spots” and therefore considered positive.

MMP1 gene expression. The skin discs were immediately flash-frozen (liquid nitrogen) after the experiment. To homogenize the tissue, the skin samples were first cut with a cryostat (25 micron sections) and placed in guanidinium thiocyanate-phenol-chloroform (1mL) (Trizol®, Life Technologies, Zug, Europe). Then, the skin sample was crushed with a series of syringes with decreasing needle diameter (19G, 20G, 25G) to completely disrupt the tissue. RNA was extracted from the homogenized sample using Trizol® (Life Technologies, Zug, Europe) following the manufacturer's protocol. RNA was re-suspended in RNAase-free water (50 μ l). The extracted RNA (1 μ g) was reverse transcribed into cDNA using the TaqMan kit transcription reverse reaction (Applied Biosystems) and hexamers (primers hazard) according to the manufacturer's protocol. Real time PCR analyses were performed using a StepOne™ machine plus (Life Technologies, Zug, Europe). Relative gene expression was analyzed with the 2⁻ $\Delta\Delta$ CT method and normalized to b-actin house keeping gene.. No adjustments were needed when certified specific MMP1 primers with a probe (MMP1 Hs00233958_m1, Actin Hs99999903_m) were used

(Life Technologies, Zug, Europe). Each reaction contained 50 ng cDNA (20 μ l), primer (1 μ l) and TaqMan Universal Master Mix II (10 μ l)(Life Technologies, Zug, Europe). We followed the standard amplification program; 20 seconds at 95 degrees, followed by 40 cycles of 1 second at 95 degrees and 20 seconds at 60 degrees.

Results

Human skin permeation. The skin permeation curves for the five PAHs after application of the PAH mixture and bitumen condensate with and without co-exposures to UV-S are shown in figure 1A and B. The skin permeation parameters are given in Table 1. The PAHs in the PAH mixture had low permeation rates (J) (0.97-13.01 ng/cm²/h), disparate lag times (T_{lag}) (1-10h), and from moderate to slow permeation coefficient (K_p). With co-exposures to UV-S, the PAHs still had low J s (0.40-6.35 ng/cm²/h); although the J s for the individual PAHs changed when co-exposed to UV-S; while T_{lag} remained unchanged and disparate (1-11h).

When the applied PAH mixture had co-exposure to UV-S, two PAHs behaved similarly with respect to simultaneous exposure to UV-S; naphthalene, and BaP, and their J s were halved (Table 1). T_{lag} increased by one hour for both. The opposite J pattern was observed for anthracene, pyrene, and chrysene where J s increased 27%, 43%, and 44%, respectively. The T_{lag} were similar as without co-exposure to UV-S (Table 1).

The PAHs in BFC had low J s (0.01-1.08 ng/cm²/h), disparate lag times (1-13.5h), and from moderate to slow K_p values. Chrysene was not detected in the reservoir liquid. With co-exposures to UV-S, the PAHs still had low J s (0.01-1.08 ng/cm²/h) although the J s for the individual PAHs changed when co-exposed to UV-S.

When the applied BFC had co-exposure to UV-S, the J s for naphthalene, anthracene, and pyrene increased compared to BFC applied without UV-S (Table 1). Large increases in J s were observed for naphthalene (300%), anthracene (600%) and pyrene (doubled). T_{lag} decreased for naphthalene (60%), anthracene (150%) and BaP (460%). The T_{lag} remained unchanged for pyrene (Table 1).

Skin biomarkers. Histopathology results from skin discs stained with HE showed no signs of irritation for the controls (undergone the same experimental treatment except for exposure). Skin exposed to UV-S for 15 minutes showed less irritation compared to skin with 40 minutes and some irritation was observed in skin exposed to the PAH mixture. Co-exposure to PAH mixture and UV-S showed appreciable amount of irritation. Some expression of p53 was observed with co-exposures to UV-S and PAHs but not with exposure to PAHs alone. The p53 expression

increased with increasing UV-S exposures (15-20 and 40 minutes) (figure 3). This increase was only seen if the skin was kept in the flow-through diffusion cells with cell culture media for 24 hours but not in saline (data not shown). We did not observe the expected up-regulation of cKIT/CD117. The choice to determine MMP-1 expression after 24 h was made based on prior experience with skin cell cultures and *in vivo* experiments (Gebbers et al. 2007; Liardet et al. 2001). However, no conclusion can be made regarding the expression of MMP-1 gene because we could not isolate sufficient RNA from the human skin, even after treating the skin with RNAase immediately after obtaining it.

Discussion

Simultaneous exposures to PAHs and UV-S increased skin permeation for all PAHs except for chrysene in BFC, and naphthalene and BaP in the PAH mixture. This increase in skin permeation when co-exposed to UV has been shown for caffeine, which increased 338% after the skin was irradiated with UVB doses above 420 mJ/cm² in a flow-through diffusion cell system *in vitro* (Gelis et al. 2002). The authors report that the skin integrity assessed by TEWL measurements was greatly different before and after UV-S exposure at this irradiation level. Below this UV dose, no difference in TEWL measurements before and after exposure was observed. This suggests that the stratum corneum was not damaged from UV-S exposure below this threshold. We cannot relate our observed differences in PAH skin permeation rates to stratum corneum damage because our experimental set-up reflected daily outdoor exposure scenarios which were far smaller than the caffeine study, with up to 60 mJ/cm², and the TEWL measurements did not change before and after experiments.

UV-S exposure decrease the intercellular strength, strain, and cell cohesion thus increasing the biomechanical driving force for damage while simultaneously decreasing the skin's natural ability to resist, compromising the critical barrier function of the skin (Biniek, Levi, and Dauskardt 2012). This could be a plausible explanation for the increase in PAH permeation we observed in our experiments, and if so, then a possible decrease in intercellular strength cannot be measured by TEWL. Indeed, cellular damages have been observed below the reported 420 mJ/cm² UV-S threshold in other studies. Keratinocytes exposed *in vitro* to UVA and UVB, separately, showed reduced plasma membrane stability, reduced proliferation and increased apoptosis compared to controls (sham-treated cells)(Larsson et al. 2005).

UVA irradiation induced loss of glutathione (GSH) in keratinocytes *in vitro* (Larsson et al. 2005). In phase I of the biotransformation, PAH epoxides are generated to convert nonpolar PAHs to polar PAHs and conjugated with glutathione in phase II of the biotransformation to facilitate excretion. Skin transplants have shown to have significant capacity for phase II metabolism including GSH conjugation (Manevski et al. 2015). However, if phase II biotransformation capacity is reduced (e.g. loss of GSH), these epoxides are converted into phenols and diols. Before these hydroxylated derivatives are conjugated and excreted, they may undergo a number of oxidation and hydroxylation reactions, converting the phenols to phenol-epoxides and subsequently to diphenols and triols, diols to tetrols and diol-epoxides, and triols to triol-epoxides and pentols as reviewed in (IARC 2010). These metabolites were not measured therefore we cannot rule out a possible underestimation of PAH skin absorption in our experiments.

PAHs absorb UV light resulting in the formation of different types of photoreaction products and lower molecular weight photodegradation products (Yu 2002). This can occur via several different photochemical reactions; oxidation to oxygenated PAHs and PAH quinones; and reaction with NO₂ or NO₃ radicals in the atmosphere to form nitro-PAHs (reviewed in (Fu et al. 2012)). The photooxidation of the parent PAHs, such as naphthalene, anthracene, pyrene, and BaP, produces hydroxylated products, PAH quinones, and ring opening products (reviewed in (Fu et al. 2012)). Predicting photodegradation products is difficult due to the ring arrangements as photochemical reactions of PAHs are highly regioselective. In general, PAHs with a higher number of benzo-fused rings exhibit greater phototoxicity (Cerniglia 1992). This phototoxicity induces lipid peroxidation in a dose-dependent manner (Botta et al. 2009). A study of UV-induced cytotoxicity for 16 PAHs (US EPA priority list) in human skin HaCaT keratinocytes showed that all, except naphthalene, exhibited phototoxicity to some extent (Wang et al. 2007). We did not reach a statistical difference between the experiments with or without UV co-exposures, as the variability introduced in experiments with UV exposure was extremely large, as can be observed from the error bars in the permeation figures. This could possibly be explained by the variable photooxidation products or the amount of phototoxicity produced, or again, that we did not measure all possible metabolites. Another explanation could be the influence of temperature on K_p. Modeled K_p values have shown that an increase in four degrees Celsius can double the K_p value (Norman et al. 2008), while experimental K_p values had a 1-28% difference when the temperature ranged from 30 to 40°C (Corley et al 2000). Thus, even small changes in temperature can increase the variability.

BaP with co-exposure to UVA have shown to produce both DNA strand breaks and oxidative lesions in human keratinocytes *in vitro* while each agent alone did not induce detectable effects (Crallan, Ingham, and Routledge 2005). The authors suggested that the ultimate BaP carcinogen - BaP diol epoxide – forms an adduct that is photosensitive and the subsequent exposure to UVA leads to DNA strand breakages; or alternatively, BaP, a photomutagenic substance itself absorbing energy in the UVA range, can become activated by UVA light and subsequently cause damage. In either of the two proposed mechanisms, BaP co-exposed to UVA irradiation would react inside the skin, thus not be detected in the reservoir liquid in the flow-through diffusion cells. Therefore, it would be false to conclude that the skin absorption was lower for BaP in the PAH mixture co-exposed with UV-S than without. This reversed pattern was not observed for BaP in BFC where BaP permeated skin to a greater extent when co-exposed to UV-S compared to without depicting the same pattern as for the other PAHs in BFC. BFC contains not only the phototoxic PAHs, but also the phototoxic nitro and sulfur heterocycle constituents. The increase in phototoxicity could potentially lead to a corresponding increase in the damage of the critical barrier function of the skin while also more of the BaP parent compounds as less photoreactive products are generated.

Naphthalene and BaP showed the same skin permeation patterns; greater permeation with UV-S exposure compared without when applied in BFC but the opposite when applied as a PAH mixture. There exist several plausible explanations for this observation; (1) Naphthalene applied as a PAH mixture evaporates faster than it is absorbed into the skin. The diffusion cell system is kept at 32°C and is equipped with jacketed cells to maintain this temperature. The solar lamp did not increase the skin surface temperature by more than 2°C; however, given naphthalene's low partial pressure (0.013 kPa at 299°K) this set-up could potentially be sufficient to evaporate the applied naphthalene from the skin. This explanation would not hold for naphthalene in BFC; (2) Naphthalene rapidly undergoes radical reactions with UV-S producing quinines that we did not measure; and /or (3) BFC exhibit a vehicle effect on naphthalene increasing the absorption across the SC. In a study of naphthalene skin absorption from jet fuel, naphthalene was quickly absorbed through the epidermis when applied to the skin in jet fuel which contains naphtha and other additives (Kim, Andersen, and Nylander-French 2006). PAH mixture in acetone as according to OECD 420 guideline does not mimic BFC in the laboratory and consequently, a possible vehicle effect would not have been taken into account.

Biomarker assessment. Never frozen, dermatomed skin flaps maintained in culture on diffusion cells have been shown to maintain their viability for at least 24 hours (Gelis et al. 2002). The UV-S doses (none, 22.5-30, and 60 mJ/cm²) presently used resulted in a dose-dependent tissue irritation as assessed according to the method of Miles et al 2014 (Miles et al. 2014). This shows the usefulness of this *in vitro* skin irritation assessment method using human viable skin and histopathology. The up-regulation of p53 increased in a dose-dependent manner with UV-S (figure 1) as have been reported previously (Latonen, Taya, and Laiho 2001). Although qualitatively assessed, the p53 up-regulation was somewhat greater after co-exposure to PAH mixture and UV-S than UV-S alone. The p53 gene functions are indicators of the genome integrity, and are activated mainly when DNA is damaged. It acts as a transcription factor that regulates several genes (cell cycle control, cell apoptosis, cell signaling, extracellular matrix control, and cell structure). This p53 up-regulation has been reported; however, in skin biopsies from workers chronically exposed to bitumen fumes (Loreto et al. 2007). This is contrary to what we observed in our study; we did not observe an up-regulation of p53 when skin was exposed to PAH (as a mixture or in BFC) without co-exposure to UV-S. The reason for the lack of p53 up-regulation in our *in vitro* experiment could be explained by a onetime exposure compared to chronic exposures. Or, the bitumen fume workers (Loreto et al. 2007) were paving roads outside thus having co-exposures to UV-S. The authors did not, however, measure UV exposure. As with the p53, we did not observe the expected down-regulation of p63. This gene, which is a p53-like gene, was found to be dramatically reduced in UV exposed keratinocytes (Liefer et al. 2000). One explanation could be the choice of antibody we used which was generated with the core DNA-binding domain that is present in all p63 isoforms thus not specific to Δ Np63a. We did not observe the expected up-regulation of cKIT/CD117 as previously seen in cultured human melanocytes exposed twice with a 48 h interval to UVB irradiation (0-80 mJ/cm²) (Hachiya et al. 2001). This up-regulation of c-KIT was measured with RT-PCR. The cKIT staining method might be sufficiently sensitive for cell cultures but not sufficiently sensitive for skin discs since most of the cells in the skin sample are keratinocytes, not melanocytes where the cKIT receptors reside. The increase in cKIT receptors from UVB stimulation might take longer than the 24 hours we ran our experiments. Another possible explanation could be that the UV-S dose used caused sufficient keratinocyte cell death (as observed as skin irritation) thereby not stimulate SCF production and ultimately no cKIT induction.

Selection of PAHs in mixture. Based on a previous study of bitumen fume exposure among road paving workers (Burstyn et al. 2002), we choose a mixture of five PAHs: naphthalene, anthracene, pyrene, chrysene, and BaP to

simulate bitumen fume exposure. Individual PAHs in bitumen fume (particulate phase) and vapor (gas phase) emitted during road paving and asphalt mixing (Burstyn et al. 2002) were quantified (mean values (standard error)) for fumes: 0.68 (0.32) $\mu\text{g}/\text{m}^3$ naphthalene, 0.18 (0.05) $\mu\text{g}/\text{m}^3$ anthracene, 0.17 (0.08) $\mu\text{g}/\text{m}^3$ pyrene, 0.09 (0.02) $\mu\text{g}/\text{m}^3$ chrysene, and 0.02 (0.01) $\mu\text{g}/\text{m}^3$ BaP; and for vapor phase: 4.65 (0.50) $\mu\text{g}/\text{m}^3$ naphthalene, 1.24 (0.20) $\mu\text{g}/\text{m}^3$ anthracene, 0.39 (0.04) $\mu\text{g}/\text{m}^3$ pyrene, 0.02 (0.003) $\mu\text{g}/\text{m}^3$ chrysene, and 0.02 (0.01) $\mu\text{g}/\text{m}^3$ BaP. The concentrations of individual PAHs in the mixture we used were a result from several tries with lower initial PAH concentrations which were below the limit of detection, making it difficult to construct permeation curves. The BFC we generated (Sutter et al. 2016) and applied to the skin, contained somewhat different individual PAH concentration ratios compared to the personal samples reported in the literature. Our BFC had lower amounts of pyrene and anthracene than measured among pavers, and this could be due to the loss of the vapor phase in our sample. The BaP concentration in our BFC was greater than previously reported in two studies (Roy, Kriech, and Mackerer 2007; Reinke et al. 2000); however, these studies measured bitumen fume emissions from storage tanks and do not reflect workplace exposures directly. We believe our experiments simulated well PAH exposures because the BFC sample was generated from bitumen obtained directly from a company paving roads in Switzerland.

PAH mixture vs BFC. Simulating bitumen exposure in the laboratory by mixing the individual PAHs normally found in bitumen did not give the same skin permeation results as the PAHs in BFC. Bitumen is the residue resulting from vacuum distillation of selected petroleum crude oils and contains many other substances such as aliphatic compounds, cyclic alkanes, aromatic hydrocarbons, heterocyclic compounds containing nitrogen, oxygen and sulfur atoms, and metals in addition to PAHs. Other organic molecules in the BFC might increase the permeation of PAHs through human skin which could explain the PAHs' much shorter timelags in BFC compared to the mixture.

Possible radical reaction products that could under estimate the total amount of PAHs absorbed remain a limitation in our study; however, we were successful in showing that the absorption of PAHs do increase with simultaneous UV-S exposures.

In conclusion, our study provides robust human skin PAH absorption estimates based on several skin donors and replicates. Although the differences between PAH exposures with co-exposures to UV or without, did not reach statistical significance, the five PAHs in the mixture were shown to have low permeation rates (0.97-13.01 $\text{ng}/\text{cm}^2/\text{h}$) and disparate lag times (1-10h). With co-exposures to UV-S, the PAHs' permeation rates remained low,

but the permeation rates increased for anthracene, pyrene and chrysene. For the PAHs in bitumen fume condensate, the permeation rates for naphthalene, anthracene, and pyrene increased with co-exposure to UVS. The vehicle matrix could potentially be the reason for this discrepancy between the PAH mixture and BFC as the latter contains additional not identified substances. We suggest using the skin flaps from permeation experiments to assess skin irritation (H&E staining) and p53 up-regulation, and continue to explore other skin biomarkers in this *in vitro* experimental set-up. To reduce the carcinogenic risks among workers exposed to PAHs and UV-S simultaneously it is recommended to increase hygienic measures such as cleaning tools and frequent hand washing to reduce skin PAH exposures, and simultaneously increase time spent in the shade (use of awnings for break times for example) and use protective clothing against sun exposures.

Acknowledgement

Funding from CRD ANSES

We would like to thank Nicole Charriere for all experimental help and Simon Desclarez, Gregory Plateel, and Philippe Boiteux († Deceased) for the chemical analysis.

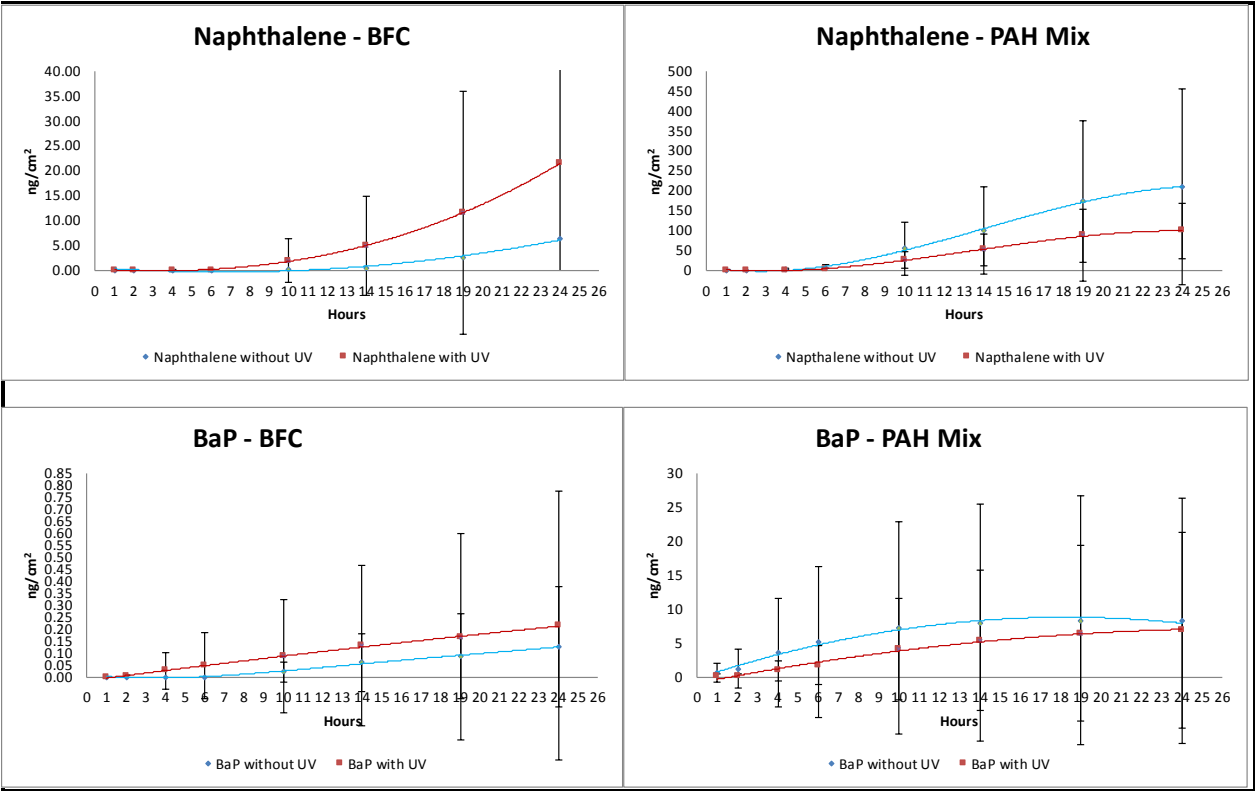


Figure 1 A Skin permeation curves and standard deviations for naphthalene and BaP in BFC (left column) and PAH mixture (right column) displaying hours of exposure (x-axis) by cumulative amount per skin area (ng/cm²) (y-axis).

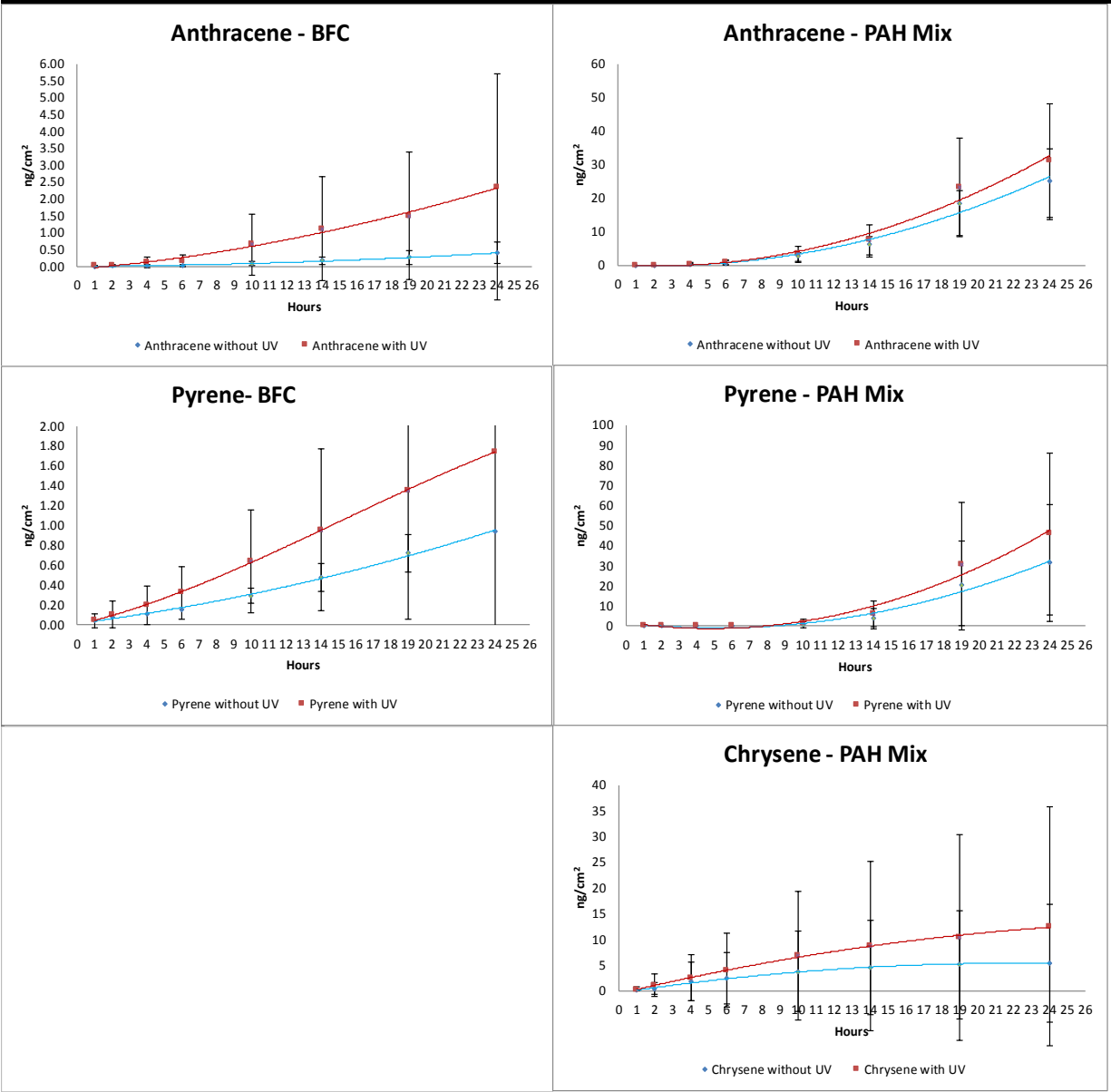


Figure 1 B Skin permeation curves and standard deviation for anthracene, pyrene, and chrysene in BFC (left column) and PAH mixture (right column) displaying hours of exposure (x-axis) by cumulative amount per skin area (ng/cm^2) (y-axis).

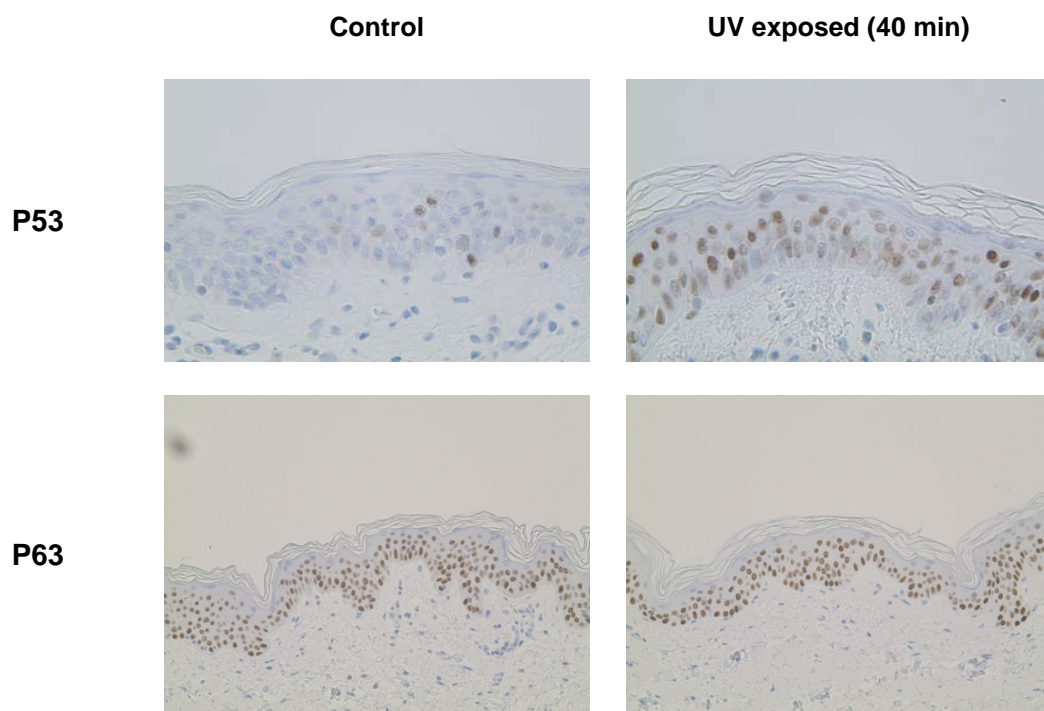


Figure 2 Examples of skin histology results; p53 (magnification 100x) and p63 (magnification 40x). Brown staining indicates presence of the antibody. A difference in p53 expression was only visible after 40 min of UV-S exposure and after 24 hrs of incubation in Dulbecco's Modified Eagle's Medium at 32°C.

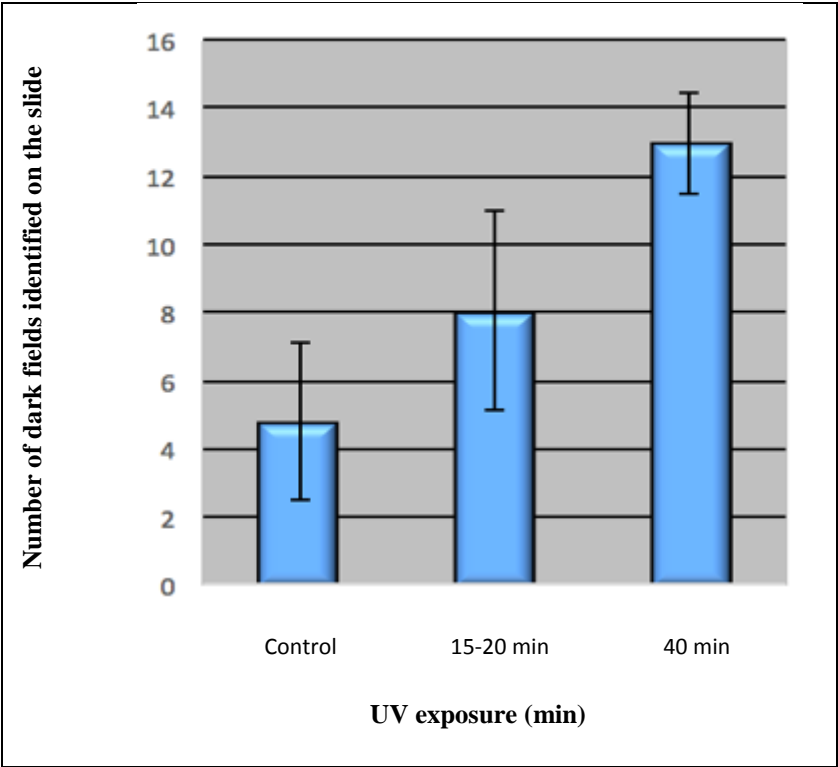


Figure 3 Expression of p53 increases with increasing UV exposure. Number of positive cells per fields identified as a measure of p53 upregulation (y-axis) and UV-S exposure times (x-axis) from four experiments (N=4 donors) in cell culture medium after 24 hours for control (no UV-S exposure) and exposed; 10-15 minutes equal to 22.5-30 mJ/cm² and 40 minutes equal to 60 mJ/cm². The error bars indicate standard deviations

Table 1 Concentrations of individual PAHs in the bitumen condensate and the PAH mixture applied to the skin (60 µl) and the resulting permeation rates (J), time lag (T_{lag}), and coefficient (K_p)

PAH	PAH mixture					Bitumen Fume Condensate				
	Start conc	J mean (SD)	T _{lag}	K _p	n	Start conc	J mean (SD)	T _{lag}	K _p	
	(ng/µl)	(ng/cm ² /h)	(h)	(cm/h)		(ng/µl)	(ng/cm ² /h)	(h)	(cm/h)	
Naphthalene	6	5000	13.01 (15.25)	5	2.60E-03	4	260	0.26 (0.29)	13.5	1.00E-03
Naphthalene + UV-S	12	5000	6.35 (5.43)	6	1.27E-03	8	260	1.08 (2.23)	8.5	4.15E-03
Anthracene	6	5000	1.73 (0.92)	5	3.46E-04	4	50	0.02 (0.02)	5	4.00E-04
Anthracene + UV-S	12	5000	2.20 (1.44)	5	4.40E-04	8	50	0.12 (0.18)	2	2.40E-03
Pyrene	6	5000	2.77 (2.40)	10	5.54E-04	4	50	0.04 (0.08)	1	8.00E-04
Pyrene + UV-S	12	5000	3.98 (3.37)	11	7.96E-04	8	50	0.08 (0.09)	1	1.60E-03
Chrysene	2	5000	1.46 (1.44)	1	2.92E-04	4	90	NA NA NA		
Chrysene + UV-S	4	5000	2.11 (1.44)	1	4.22E-04	8	90	NA NA NA		
BaP	6	5000	0.97 (2.09)	1	1.94E-04	4	60	0.01 (0.01)	7	1.67E-04
BaP + UV-S	12	5000	0.40 (0.66)	1.5	8.00E-05	8	60	0.01 (0.02)	1.5	1.67E-04

NA Not Available – no chrysene was detected in the reservoir fluid

References

- Bolliet C, Kriech AJ, Juery C, Vaissiere M, Brinton MA, Osborn LV. (2015). Effect of Temperature and Process on Quantity and Composition of Laboratory-generated Bitumen Emissions. *J Occup Environ Hyg*; 12 438–449. doi:10.1080/15459624.2015.1009982
- Binet S, Pfohl-Leszkoicz A, Brandt H, Lafontaine M, Castegnaro M. (2002) Bitumen fumes: review of work on the potential risk to workers and the present knowledge on its origin. *Sci Total Environ*; 300 37-49.
- Biniek K, Levi K, Dauskardt RH. (2012) Solar UV radiation reduces the barrier function of human skin. *Proc Natl Acad Sci U S A*; 109 17111-6.
- Botta C, Di Giorgio C, Sabatier AS, De Meo M. (2009) Effects of UVA and visible light on the photogenotoxicity of benzo[a]pyrene and pyrene. *Environ Toxicol*; 24 492-505.
- Burke KE, Wei H. (2009) Synergistic damage by UVA radiation and pollutants. *Toxicol Ind Health*; 25 219-24.
- Burstyn I, Randem B, Lien JE, Langard S, Kromhout H. (2002) Bitumen, polycyclic aromatic hydrocarbons and vehicle exhaust: exposure levels and controls among Norwegian asphalt workers. *Ann Occup Hyg*; 46 79-87.
- Cavallari JM, Zwack LM, Lange CR, Herrick RF, McClean MD. (2012) Temperature-Dependent Emission Concentrations of Polycyclic Aromatic Hydrocarbons in Paving and Built-Up Roofing Asphalts. *Ann Occup Hyg*; 56 148–160. doi:10.1093/annhyg/mer107
- Cerniglia CE. (1992) Biodegradation of polycyclic aromatic hydrocarbons. *Biodegradation*; 3 351-68.
- Corley RA, Gordon SM, Wallace LA. (2000) Physiologically based pharmacokinetic modeling of the temperature-dependent dermal absorption of chloroform by humans following bath water exposures. *Toxicol Sci*; 53 12-23.
- Crallan RA, Ingham E, Routledge MN. (2005) Wavelength dependent responses of primary human keratinocytes to combined treatment with benzo[a]pyrene and UV light. *Mutagenesis*; 20 305-10.
- Diffey BL. (2002) Sources and measurement of ultraviolet radiation. *Methods*; 28 4-13.
- Fonseca FV, Tomasich FD, Jung JE, Maestri CA, Carvalho NS. (2016) The role of P16ink4a and P53 immunostaining in predicting recurrence of HG-CIN after conization treatment. *Rev Col Bras Cir*; 43 35-41.
- Fu PP, Xia Q, Sun X, Yu H. (2012) Phototoxicity and environmental transformation of polycyclic aromatic hydrocarbons (PAHs)-light-induced reactive oxygen species, lipid peroxidation, and DNA damage. *J Environ Sci Health C Environ Carcinog Ecotoxicol Rev*; 30 1-41.
- Garssen J, van Loveren H. (2001) Effects of ultraviolet exposure on the immune system. *Crit Rev Immunol*; 21 359-97.
- Gebbers N, Hirt-Burri N, Scaletta C, Hoffmann G, Applegate LA. (2007) Water-filtered infrared-A radiation (wIRA) is not implicated in cellular degeneration of human skin. *Ger Med Sci*; 5 Doc08.
- Gelis C, Mavon A, Delverdiere M, Paillous N, Vicendo P. (2002) Modifications of in vitro skin penetration under solar irradiation: evaluation on flow-through diffusion cells. *Photochem Photobiol*; 75 598-604.
- Hachiya A, Kobayashi A, Ohuchi A, Takema Y, Imokawa G. (2001) The paracrine role of stem cell factor/c-kit signaling in the activation of human melanocytes in ultraviolet-B-induced pigmentation. *J Invest Dermatol*; 116 578-86.
- Huynh CK, Duc TV, Deygout F, Le Coutaller P, Surmont F. (2007) Identification and quantification of PAH in bitumen by GC-ion-MS and HPLC-fluorescent detectors. *Polycyclic Aromatic Compounds*; 27 107-21.
- IARC. (1992) Solar and Ultraviolet Radiation. Lyon, France: International Agency for Research on Cancer.
- IARC. (2010) Some non-heterocyclic polycyclic aromatic hydrocarbons and some related exposures. Lyon, France: International Agency for Research on Cancer.
- IARC. (2013) Bitumen and bitumen emissions, and some N- and S-heterocyclic aromatic hydrocarbons. Lyon, France: International Agency for Research on Cancer.
- Kim D, Andersen ME, Nylander-French LA. (2006) Dermal absorption and penetration of jet fuel components in humans. *Toxicol Lett*; 165 11-21.
- Lahmann C, Young AR, Wittern KP, Bergemann J. (2001) Induction of mRNA for matrix metalloproteinase 1 and tissue inhibitor of metalloproteinases 1 in human skin in vivo by solar simulated radiation. *Photochem Photobiol*; 73 657-63.
- Lange CR, Stroup-Gardiner M. (2007) Temperature-Dependent Chemical-Specific Emission Rates of Aromatics and Polyaromatic Hydrocarbons (PAHs) in Bitumen Fume. *J Occup Environ Hyg*; 4 72–76. doi:10.1080/15459620701385279
- Larsson P, Andersson E, Johansson U, Ollinger K, Rosdahl I. (2005) Ultraviolet A and B affect human melanocytes and keratinocytes differently. A study of oxidative alterations and apoptosis. *Exp Dermatol*; 14 117-23.
- Latonen L, Taya Y, Laiho M. (2001) UV-radiation induces dose-dependent regulation of p53 response and modulates p53-HDM2 interaction in human fibroblasts. *Oncogene*; 20 6784-93.
- Liardet S, Scaletta C, Panizzon R, Hohlfeld P, Laurent-Applegate L. (2001) Protection against pyrimidine dimers, p53, and 8-hydroxy-2'-deoxyguanosine expression in ultraviolet-irradiated human skin by sunscreens: difference between UVB + UVA and UVB alone sunscreens. *J Invest Dermatol*; 117 1437-41.
- Liefer KM, Koster MI, Wang XJ, Yang A, McKeon F, Roop DR. (2000) Down-regulation of p63 is required for epidermal UV-B-induced apoptosis. *Cancer Res*; 60 4016-20.

- Liu Z, Lu Y, Rosenstein B, Lebwohl M, Wei H. (1998) Benzo[a]pyrene enhances the formation of 8-hydroxy-2'-deoxyguanosine by ultraviolet A radiation in calf thymus DNA and human epidermoid carcinoma cells. *Biochemistry*; 37 10307-12.
- Loreto C, Rapisarda V, Carnazza ML, Musumeci G, D'Agata V, Valentino M, Martinez G. (2007) Bitumen products alter bax, bcl-2 and cytokeratin expression: an in vivo study of chronically exposed road pavers. *J Cutan Pathol*; 34 699-704.
- Manevski N, Swart P, Balavenkatraman KK, Bertschi B, Camenisch G, Kretz O, Schiller H, Walles M, Ling B, Wettstein R, *et al.* (2015) Phase II metabolism in human skin: skin explants show full coverage for glucuronidation, sulfation, N-acetylation, catechol methylation, and glutathione conjugation. *Drug Metab Dispos*; 43 126-39.
- Miles A, Berthet A, Hopf NB, Gilliet M, Raffoul W, Vernez D, Spring P. (2014) A new alternative method for testing skin irritation using a human skin model: a pilot study. *Toxicol In Vitro*; 28 240-7.
- Mills AA, Zheng B, Wang XJ, Vogel H, Roop DR, Bradley A. (1999) p63 is a p53 homologue required for limb and epidermal morphogenesis. *Nature*; 398 708-13.
- Milon A, Sottas P-E, Bulliard J-L, Vernez D. (2007) Effective exposure to solar UV in building workers: influence of local and individual factors. *J Expo Sci Environ Epidemiol*; 17 58-68.
- Normann AM, Kissel JC, Shirai JH, Smith JA, Stumbaugh KL, Bunge A. (2008) Effect of PBPK model structure on interpretation of in vivo human aqueous dermal exposure trials. *Toxicol Sci*; 104 210-217
- Perlow RA, Kolbanovskii A, Hingerty BE, Geacintov NE, Broyde S, Scicchitano DA. (2002) DNA adducts from a tumorigenic metabolite of benzo[a]pyrene block human RNA polymerase II elongation in a sequence- and stereochemistry-dependent manner. *J Mol Biol*; 321 29-47.
- Pinnagoda J, Tupker RA, Agner T, Serup J. (1990) Guidelines for transepidermal water loss (TEWL) measurement. A report from the Standardization Group of the European Society of Contact Dermatitis. *Contact Dermatitis*; 22 164-78.
- Rass K, Reichrath J. (2008) UV damage and DNA repair in malignant melanoma and nonmelanoma skin cancer. *Adv Exp Med Biol*; 624 162-78.
- Reinke G, Swanson M, Paustenbach D, Beach J. (2000) Chemical and mutagenic properties of asphalt fume condensates generated under laboratory and field conditions. *Mutat Res*; 469 41-50.
- Roskoski R, Jr. (2005) Signaling by Kit protein-tyrosine kinase--the stem cell factor receptor. *Biochem Biophys Res Commun*; 337 1-13.
- Roy TA, Kriech AJ, Mackerer CR. (2007) Percutaneous Absorption of Polycyclic Aromatic Compounds from Bitumen Fume Condensate. *Journal of Occupational and Environmental Hygiene*; 4:S1 137-43.
- Saladi R, Austin L, Gao D, Lu Y, Phelps R, Lebwohl M, Wei H. (2003) The combination of benzo[a]pyrene and ultraviolet A causes an in vivo time-related accumulation of DNA damage in mouse skin. *Photochem Photobiol*; 77 413-9.
- Scharffetter K, Wlaschek M, Hogg A, Bolsen K, Schothorst A, Goerz G, Krieg T, Plewig G. (1991) UVA irradiation induces collagenase in human dermal fibroblasts in vitro and in vivo. *Arch Dermatol Res*; 283 506-11.
- Senoo M, Pinto F, Crum CP, McKeon F. (2007) p63 is essential for the proliferative potential of stem cells in stratified epithelia. *Cell*; 129 523-36.
- Shyong EQ, Lu Y, Goldstein A, Lebwohl M, Wei H. (2003) Synergistic enhancement of H₂O₂ production in human epidermoid carcinoma cells by Benzo[a]pyrene and ultraviolet A radiation. *Toxicol Appl Pharmacol*; 188 104-9.
- Sutter B, Ravera C, Hussard C, Langlois E. (2016) Alternatives for Benzene in the Extraction of Bitumen Fume from Exposure Sample Media. *Ann Occup Hyg*; 60 101-12.
- Wang S, Sheng Y, Feng M, Leszczynski J, Wang L, Tachikawa H, Yu H. (2007) Light-induced cytotoxicity of 16 polycyclic aromatic hydrocarbons on the US EPA priority pollutant list in human skin HaCaT keratinocytes: relationship between phototoxicity and excited state properties. *Environ Toxicol*; 22 318-27.
- Wang Y, Saladi R, Wei H. (2003) Synergistic carcinogenesis of chemical carcinogens and long wave-length UVA radiation. *Trends in Photochem & Photobio*; 10 31-45.
- Yang A, Kaghad M, Wang Y, Gillett E, Fleming MD, Dotsch V, Andrews NC, Caput D, McKeon F. (1998) p63, a p53 homolog at 3q27-29, encodes multiple products with transactivating, death-inducing, and dominant-negative activities. *Mol Cell*; 2 305-16.
- Yoshida H, Kunisada T, Grimm T, Nishimura EK, Nishioka E, Nishikawa SI. (2001) Review: melanocyte migration and survival controlled by SCF/c-kit expression. *J Investig Dermatol Symp Proc*; 6 1-5.
- Yu H. (2002) Environmental carcinogenic polycyclic aromatic hydrocarbons: photochemistry and phototoxicity. *J Environ Sci Health C Environ Carcinog Ecotoxicol Rev*; 20 149-83.